Acta Crystallographica Section F
Structural Biology and Crystallization Communications
ISSN 1744-3091

Crystallization and preliminary X-ray diffraction studies of hexokinase KlHxk1 from *Kluyveromyces lactis*

E. Bartholomeus Kuettner,[a]‡ Thomas M. Kriegel,[b]*‡ Antje Keim,[a] Manfred Naumann[c] and Norbert Sträter[a]*

[a]Biotechnologisch-Biomedizinisches Zentrum, Institut für Bioanalytische Chemie, Fakultät für Chemie und Mineralogie, Universität Leipzig, Deutscher Platz 5, D-04103 Leipzig, Germany, [b]Technische Universität Dresden, Medizinische Fakultät Carl Gustav Carus, Institut für Physiologische Chemie, Fetscherstrasse 74, D-01307 Dresden, Germany, and [c]Institut für Biochemie, Medizinische Fakultät, Universität Leipzig, Johannisallee 30, D-04103 Leipzig, Germany

‡ These authors contributed equally to this work.

Correspondence e-mail: kriegel@mail.zih.tu-dresden.de, strater@bbz.uni-leipzig.de

Received 23 January 2007
Accepted 12 April 2007

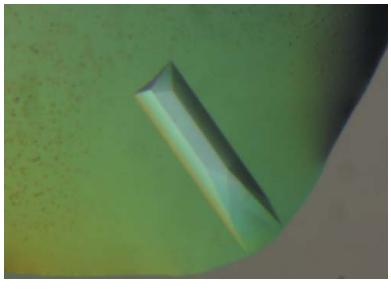

Glucose acts as both a carbon source and a hormone-like regulator of gene expression in eukaryotic organisms from yeast to man. Phosphorylation of glucose is executed by hexokinases, which represent a class of multifunctional enzymes that, in addition to their contribution to the uptake and initiation of metabolism of glucose, fructose and mannose, are involved in glucose signalling. The genome of the budding yeast *Kluyveromyces lactis* encodes a single hexokinase (KlHxk1) and a single glucokinase (KlGlk1). KlHxk1 exists in a monomer–homodimer equilibrium which is presumed to play a role in metabolic regulation. In order to evaluate the physiological significance of KlHxk1 dimerization on a molecular level, the enzyme was crystallized and subjected to X-ray structure analysis. Crystallization employing ammonium sulfate, diammonium phosphate or polyethylene glycol 6000 at pH values of 8.0–9.5 gave seven different crystal forms of KlHxk1. Crystallographic data to 1.66 Å resolution were obtained using synchrotron radiation. Structure determination of KlHxk1 in various packing environments will reveal the full architecture of the homodimeric enzyme and complete our mechanistic understanding of the catalytic and regulatory functions of the enzyme.

1. Introduction

Hexokinases are key enzymes in the metabolism of glucose, fructose and mannose. They are also involved in glucose signalling in eukaryotes from yeast to man, including plants (Entian, 1980; Rolland *et al.*, 2001, 2006; Wilson, 2003). The budding yeast *Saccharomyces cerevisiae* has three 'genuine' glucose kinases (ScHxk1, ScHxk2 and ScGlk1) encoded by the genes *ScHXK1*, *ScHXK2* and *ScGLK1*, respectively. Expression of any of these kinases alone is sufficient to allow growth on glucose (Lobo & Maitra, 1977). In contrast, the glucokinase paralogue *ScEMI2* (**E**arly **M**eiotic **I**nduction; Enyenihi & Saunders, 2003) encodes a protein which, although exhibiting 72% identity to ScGlk1, is apparently unable to support glucose utilization of a *hxk1 hxk2 glk1* triple kinase mutant of *S. cerevisiae* (Vojtek & Fraenkel, 1990). Isoenzyme ScHxk2 regulates the expression of *ScHXK1* and *ScGLK1* (Rodriguez *et al.*, 2001) and plays a prominent role in glucose sensing and glucose repression (Moreno *et al.*, 2005). Glucose limitation results in phosphorylation of ScHxk2 at Ser14 *in vivo* (Kriegel *et al.*, 1994), causing dissociation of the homodimeric enzyme *in vitro* (Behlke *et al.*, 1998). Monomeric ScHxk2 shows increased substrate affinity and, in contrast to the dimeric enzyme, is inhibited by free adenosine 5′-triphosphate (ATP) at physiological concentrations (Golbik *et al.*, 2001). ScHxk2 interacts *via* residues 6–15 with the repressor protein ScMig1 to form a complex that mediates glucose repression in the nucleus (Moreno *et al.*, 2005). The significance of phosphorylation of Ser14 and dissociation of the homodimeric enzyme to form ScHxk2–ScMig1, however, has not yet been experimentally addressed.

The existence of three glucose-phosphorylating enzymes (ScHxk1, ScHxk2 and ScGlk1) and one glucokinase-like protein (ScEmi2) in *S. cerevisiae* reflects genetic redundancy resulting from a whole genome-duplication event in the evolutionary history of the genus *Saccharomyces* (Wolfe & Shields, 1997; Seoighe & Wolfe, 1999). In

contrast, the genome of *Kluyveromyces lactis* which did not undergo duplication encodes a single hexokinase (KlHxk1; Bär *et al.*, 2003) and a single glucokinase (KlGlk1; Kettner *et al.*, 2007). Monomeric KlHxk1 has a molecular weight of about 53 kDa and shares 70% and 73% sequence identity and 84% and 85% sequence similarity with ScHxk1 and ScHxk2, respectively. The enzyme predominantly exists as a homodimer at protein concentrations higher than 1 mg ml^{-1} (Bär *et al.*, 2003). Unlike ScHxk2, glucose phosphorylation by KlHxk1 is not inhibited by free ATP at cellular levels of the nucleotide (Bär *et al.*, 2003). Interestingly, autophosphorylation of KlHxk1, presumably affecting serine residue 156, only results in partial inactivation of the enzyme (Bär *et al.*, 2003), while ScHxk2 is completely inactivated by autophosphorylation of the equivalent residue Ser157, which is located in the immediate vicinity of the active site (Heidrich *et al.*, 1997). Despite significant progress in the understanding of the catalytic and regulatory functions of hexokinases at the molecular level, no high-resolution dimer structure of any yeast hexokinase has been reported to date. Structure determination of the KlHxk1 homodimer is expected to provide the molecular data required to obtain novel insights into the control of enzyme conformation, catalytic activity and interaction with cytosolic and nuclear proteins of *K. lactis* by modulation of the monomer–homodimer equilibrium.

2. Materials and methods

2.1. Expression and purification

Cloning and overexpression of the *RAG5* gene encoding *K. lactis* hexokinase KlHxk1 (Rag5p), as well as purification of the KlHxk1 enzyme, was performed as described by Bär *et al.* (2003). Prior to crystallization, the purified enzyme was equilibrated on a HiLoad 16/60 Superdex 200 prep-grade column (GE Healthcare, Munich, Germany) with 10 m*M* Tris buffer containing 1 m*M* EDTA, 1 m*M* DL-dithiothreitol and 0.5 m*M* phenylmethanesulfonyl fluoride pH 7.4. The eluted protein was concentrated in VivaSpin-20 or VivaSpin-6 tubes with a molecular-weight cut-off limit of 10 kDa at 277 K to a protein concentrations of 10–14 mg ml^{-1}. The protein concentration was determined according to Bradford (1976) using bovine serum albumin fraction V (Lot 3X04340; Applichem, Darmstadt, Germany) as a standard.

2.2. Crystallization

Tailor-made sparse-matrix screens (Jancarik & Kim, 1991) adapted from commercially available crystallization screens from Hampton Research (Aliso Viejo, CA, USA) and Jena BioScience (Jena, Germany) were performed at 292 K using the sitting-drop vapour-diffusion technique in three-drop 96-well Greiner plates with a hydrophobic surface in order to determine initial crystallization conditions. The volume of the reservoir solution was 82 µl. Equal volumes (0.2 µl) of reservoir and protein solution were dispensed using a Cartesian eight-channel dispensing system (Genomic Solutions, Irvine, CA, USA). Further optimization at 292 K was performed employing the hanging-drop technique in 24-well plates (two 12-well PVC trays; Nelipak Venray, The Netherlands) and polystyrene tray boxes (VWR, Darmstadt, Germany) using AquaSil-siliconized (Hampton Research, Aliso Viejo, CA, USA) cover slides (Roth, Karlsruhe, Germany). The volume of the reservoir solution was 500 µl. For the hanging drop, 1 µl reservoir buffer was mixed with 1 µl protein solution. Crystals of rod-like, plate-like or compact shape (Fig. 1) were obtained using ammonium sulfate, diammonium hydrogen phosphate, polyethylene glycol (PEG) of molecular weight 6000 Da and LiCl as precipitants (Table 1). Crystals appeared within a few days and usually reached their final size within 1–4 weeks (Table 1).

2.3. Data collection and processing

For cryo data collection, crystals mounted in a rayon loop (Hampton Research, Aliso Viejo, CA, USA) were either incubated for 1–2 s in dry paraffin oil (Riboldi-Tunnicliffe & Hilgenfeld, 1999)

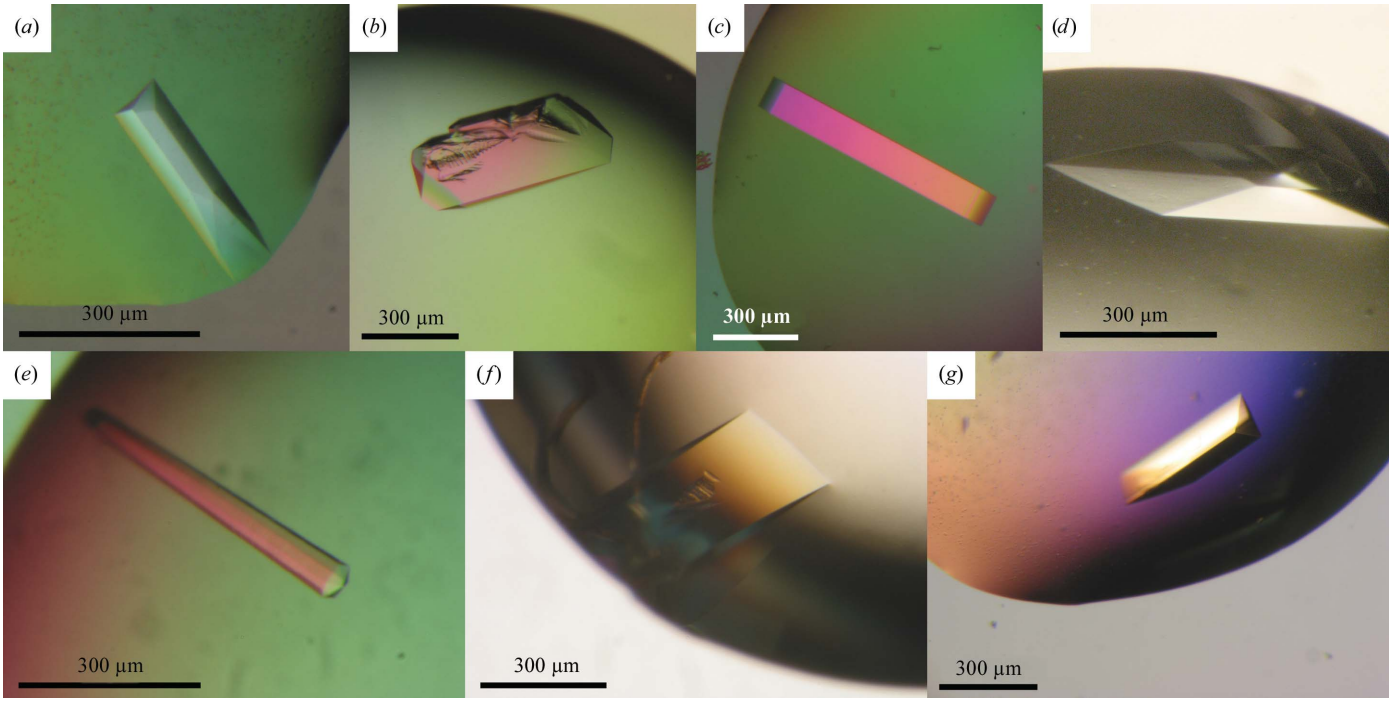

Figure 1
Crystals of KlHxk1. Detailed crystallization conditions are listed in Table 1.

Table 1
Crystal data and data-collection statistics of crystals grown at 292 K.

Crystal form	I (Fig. 1*a*)	II (Fig. 1*b*)	III (Fig. 1*c*)	IV (Fig. 1*d*)	V (Fig. 1*e*)	VI (Fig. 1*f*)	VII (Fig. 1*g*)
Reservoir solution	2.4–2.6 *M* $(NH_4)_2SO_4$, 0.1 *M* CHES† pH 9.3–9.5	22% PEG 6000, 0.1 *M* Tris pH 8.0	2.0–2.6 *M* $(NH_4)_2HPO_4$, 0.1 *M* CHES pH 9.2–9.8	2.5 *M* $(NH_4)_2SO_4$, 0.1 *M* CHES pH 9.5	20–24% PEG 6000, 0.1 *M* Tris pH 8.0	18–26% PEG 6000, 0.1 *M* Bicine pH 9.0	2.6 *M* $(NH_4)_2SO_4$, 0.1 *M* CHES pH 9.4
Cryocooling condition	Paraffin oil	(298 K)	20%(*v*/*v*) glycerol	10%(*v*/*v*) glycerol	(298 K)	+4% PEG 6000, 20%(*v*/*v*) ethylene glycol	(298 K)
X-ray source	Rotating anode	Rotating anode	BESSY BL14.3	Rotating anode	Rotating anode	Rotating anode	Rotating anode
Wavelength (Å)	1.5418	1.5418	0.9537	1.5418	1.5418	1.5418	1.5418
Data-collection temperature (K)	100	298	100/298‡	100	298	100	298
Space group§	$P2_12_12$	$C2$	$P2_1$	$P2_1$	$P6_x$	$P2_x$	$P2_12_12$
Resolution limit (Å)	2.4	2.8	1.66/3.2	2.0	3.3	1.9	3.3
Unit-cell parameters							
a (Å)	98.9	144.5	60.3/61.6	73.8	137.1	92.5	100.2
b (Å)	113.4	57.0	135.8/138.5	92.1	137.1	98.4	122.7
c (Å)	91.3	72.8	72.6/73.1	92.6	107.0	115.0	93.5
β (°)		110.3	92.1/92.5	111.0		95.8	
V_M (Å^3 Da^{-1})	2.4	2.7	2.8/2.9	2.8	2.7	2.4	2.7
Solvent content (%)	49	53	56/58	56	55	49	55
Molecules per ASU	2	1	2	2	2	2	2
Total reflections	580367	24381	688456	594606	n.d.	n.d.	30538
Unique reflections	40831	11502	129723	71898	n.d.	n.d.	14143
Completeness (%)	99.9 (99.7)	82.7 (62.4)	94.5 (95.3)	92.0 (97.7)	n.d.	n.d.	79.2 (72.9)
R_{sym}¶	7.6 (24.8)	6.7 (17.1)	5.0 (48.5)	5.8 (23.0)	n.d.	n.d.	15.5
$R_{p.i.m.}$††	2.1 (12.8)	5.0 (15.2)	2.3 (23.6)	2.1 (17.5)	n.d.	n.d.	37.6

† CHES, *N*-cyclohexyl-2-aminoethanesulfonic acid. ‡ Unit-cell parameters and the V_M values correspond to data sets at the two given temperatures. Data-processing statistics are only listed for the synchrotron data collected at 100 K. § *x*, possible screw axes could not be determined owing to insufficient data. ¶ $R_{sym} = \sum_{hkl}\sum_i |I(hkl) - \langle I(hkl)\rangle| / \sum_{hkl}\sum_i I(hkl)$. †† $R_{p.i.m.} = \sum_{hkl}[1/(N-1)]^{1/2}\sum_i |I(hkl) - \langle I(hkl)\rangle| / \sum_{hkl}\sum_i I(hkl)$. $R_{p.i.m.}$ describes the precision of merged reflections by incorporation of the multiplicity *N* (Weiss, 2001).

or transferred to the reservoir buffer used for crystallization supplemented with glycerol or ethylene glycol to final concentrations of up to 10–20%(*v*/*v*). X-ray data sets were collected from crystal forms I, III and IV using an in-house rotating-anode generator (Bruker-AXS MicroStar, Karlsruhe, Germany) or using synchrotron radiation (beamline BL14.3 of BESSY and Free University Berlin at BESSY in Berlin, Germany) (Table 1). Specimens of crystal forms II, V and VII were transferred to a quartz capillary (Müller, Schönwalde, Germany) in order to collect room-temperature data. The resolution limit given in Table 1 was chosen such that the signal-to-noise ratio was larger than 2 and R_{sym} was lower than about 50% for the highest resolution shell. Processing and scaling of diffraction images was performed using programs from the *HKL* package (v.1.96.5 and v.1.97.2; Otwinowski & Minor, 1997) and the program *RMERGE* (Weiss, 2001). Further data processing (Table 1) was conducted employing the programs *SCALEPACK2MTZ*, *CAD* (Collaborative Computational Project, Number 4, 1994) and *TRUNCATE* (French & Wilson, 1978).

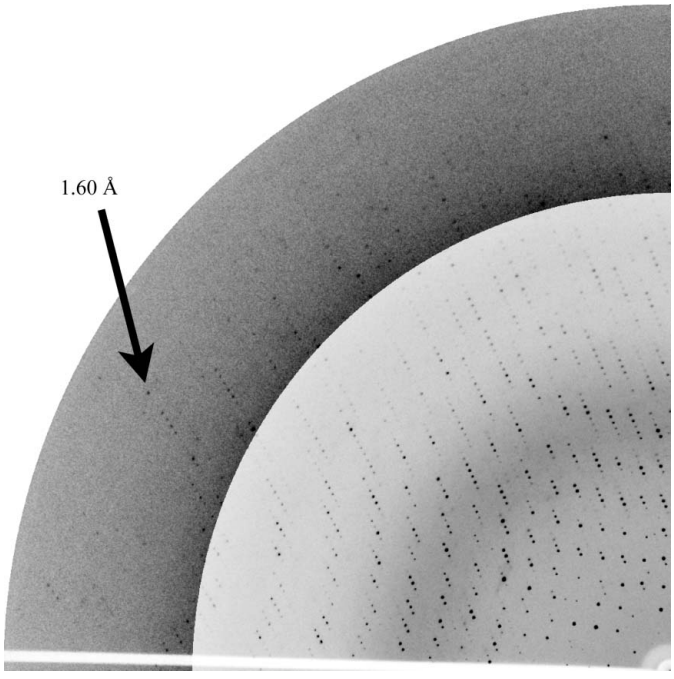

Figure 2
X-ray diffraction pattern of KlHxk1 crystal form III. A quarter wedge of the diffraction image is shown, with the high-resolution section made darker in order to clearly visualize reflections. The arrow marks a spot at 1.60 Å resolution.

3. Results and discussion

The enzyme KlHxk1 (Rag5p) from *K. lactis* was first crystallized in an orthorhombic space group at 292 K using ammonium sulfate as the precipitant at pH 9.5 (Fig. 1*a*, Table 1, crystal form I). The same crystal form also grew in the presence of 20% PEG 6000 at pH 9.0 (0.1 *M* Bicine), but with a crystallization time of several months. The monoclinic crystal form IV (Fig. 1*d*) was obtained under the conditions described for crystal form I (Table 1). It showed a more plate-like shape compared with the rod-like shape of crystal form I (Figs. 1*a* and 1*d*). In the presence of ammonium sulfate, a second orthorhombic crystal form (VII) with similar habit and unit-cell parameters but an increased length of the *b* axis by about 9 Å was obtained (Table 1). Another salt precipitant, ammonium phosphate, only produced monoclinic crystals at high pH (Table 1, crystal form III). Crystal form VII was also obtained in the presence of 0.9 *M* LiCl together with 18% PEG 6000 at pH 8 (0.1 *M* Tris). Crystal forms I and VII may be related to each other since they exhibit the same space group and have similar unit-cell parameters. Crystal form VI shows unit-cell parameters that are close to those of form I, but reveals lower symmetry. The best resolution was obtained for crystal form III using synchrotron radiation (Fig. 2).

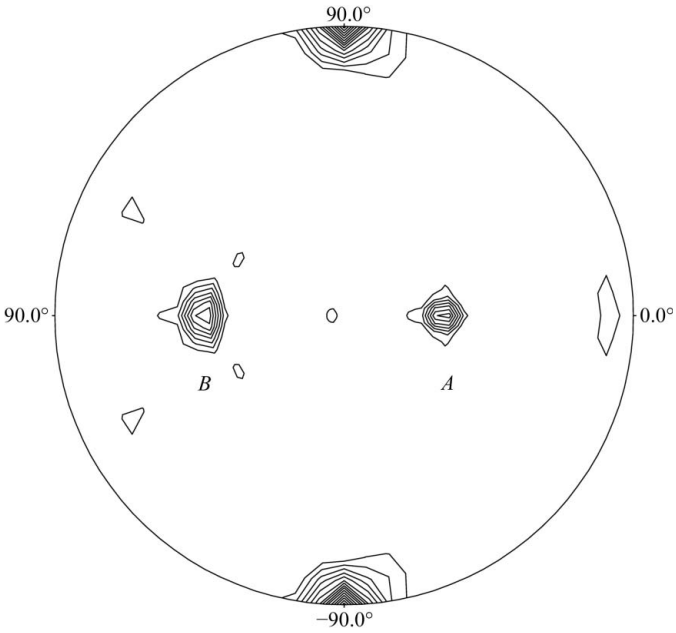

Figure 3
Self-rotation function of crystal form III calculated using the program *POLARRFN* (Collaborative Computational Project, Number 4, 1994) with an integration radius of 36 Å and to a resolution of 5.0 Å. Peaks of more than 3 root-mean square deviations (r.m.s.d.s) are shown and are contoured by an increment of 1 r.m.s.d. The depicted section is at $\kappa = 180^\circ$ and has $\omega = 0$ or 180° at the centre of the image and $\omega = 90^\circ$ around the edge. φ is marked around the periphery.

A self-rotation function has been calculated for crystal form III (Fig. 3). Two noncrystallographic peaks are visible in the $\kappa = 180^\circ$ (twofold rotation axis) section. Further analysis shows that this crystal contains two monomers in the asymmetric unit and that the peak labelled *A* corresponds to twofold symmetry of the dimer axis, whereas peak *B* reflects a noncrystallographic twofold rotation between two dimers.

The large number of crystal forms and the crystallographic resolution make it appropriate to perform comparative crystal-packing and protein-conformation analyses in order to explore the molecular basis of catalysis and metabolic regulation by KlHxk1. Since the enzyme oligomerizes reversibly at relatively high enzyme concentrations, the dimer interface is unlikely to be significantly larger than the interfaces formed by packing interactions in the crystal. Therefore, a comparison of different crystal forms may help to identify the physiological dimer which is ideally present in all crystal forms. In addition, a comparison of the different enzyme conformers which form under the influence of different packing interactions and bound substrates or inhibitors will allow exploration of the domain mobility of the enzyme. For yeast hexokinases, domain mobility seems to represent a basic prerequisite for enzyme function, since a domain movement is thought to be part of their catalytic cycle (Steitz *et al.*, 1981; Kuser *et al.*, 2000).

The authors thank Uwe Müller and Martin Fieber-Erdmann from Protein Structure Factory at BESSY (Berlin) for their help and assistance during synchrotron data collection and Karina Kettner (Dresden University of Technology) for support during enzyme purification.

References

Bär, D., Golbik, R., Hübner, G., Lilie, H., Müller, E. C., Naumann, M., Otto, A., Reuter, R., Breunig, K. D. & Kriegel, T. M. (2003). *J. Biol. Chem.* **278**, 39280–39286.
Behlke, J., Heidrich, K., Naumann, M., Müller, E.-C., Otto, A., Reuter, R. & Kriegel, T. (1998). *Biochemistry*, **37**, 11989–11995.
Bradford, M. M. (1976). *Anal. Biochem.* **72**, 248–254.
Collaborative Computational Project, Number 4 (1994). *Acta Cryst.* D**50**, 760–763.
Entian, K. D. (1980). *Mol. Gen. Genet.* **178**, 633–637.
Enyenihi, A. H. & Saunders, W. S. (2003). *Genetics*, **163**, 47–54.
French, S. & Wilson, K. S. (1978). *Acta Cryst.* A**34**, 517–527.
Golbik, R., Naumann, M., Otto, A., Müller, E.-C., Behlke, J., Reuter, R., Hübner, G. & Kriegel, T. M. (2001). *Biochemistry*, **40**, 1083–1090.
Heidrich, K., Otto, A., Behlke, J., Rush, J., Wenzel, K. W. & Kriegel, T. (1997). *Biochemistry*, **36**, 1960–1964.
Jancarik, J. & Kim, S.-H. (1991). *J. Appl. Cryst.* **24**, 409–411.
Kettner, K., Müller, E.-C., Otto, A., Rödel, G., Breunig, K. D. & Kriegel, T. M. (2007). In the press.
Kriegel, T. M., Rush, J., Vojtek, A. B., Clifton, D. & Fraenkel, D. G. (1994). *Biochemistry*, **33**, 148–152.
Kuser, P. R., Krauchenco, S., Antunes, O. A. C. & Polikarpov, I. (2000). *J. Biol. Chem.* **275**, 20814–20821.
Lobo, Z. & Maitra, P. K. (1977). *Arch. Biochem. Biophys.* **182**, 639–645.
Moreno, F., Ahuatzi, D., Riera, A., Palomino, C. A. & Herrero, P. (2005). *Biochem. Soc. Trans.* **33**, 265–268.
Otwinowski, Z. & Minor, W. (1997). *Methods Enzymol.* **276**, 307–326.
Riboldi-Tunnicliffe, A. & Hilgenfeld, R. (1999). *J. Appl. Cryst.* **32**, 1003–1005.
Rodriguez, A., De La Cera, T., Herrero, P. & Moreno, F. (2001). *Biochem J.* **355**, 625–631.
Rolland, F., Baena-Gonzalez, E. & Sheen, J. (2006). *Annu. Rev. Plant Biol.* **57**, 675–709.
Rolland, F., Winderickx, J. & Thevelein, J. M. (2001). *Trends Biochem. Sci.* **26**, 310–317.
Seoighe, C. & Wolfe, K. H. (1999). *Curr. Opin. Microbiol.* **2**, 548–554.
Steitz, T. A., Shoham, M. & Bennett, W. S. Jr (1981). *Philos. Trans. R. Soc. Lond. B Biol. Sci.* **293**, 43–52.
Vojtek, A. B. & Fraenkel, D. G. (1990). *Eur. J. Biochem.* **190**, 371–375.
Weiss, M. S. (2001). *J. Appl. Cryst.* **34**, 130–135.
Wilson, J. E. (2003). *J. Exp. Biol.* **206**, 2049–2057.
Wolfe, K. H. & Shields, D. C. (1997). *Nature (London)*, **387**, 708–713.